

변분적 점근법을 사용한 이중 세포를 갖는 박벽보의 모델링

박재상* · 김지환*

Modeling of two-cell thin-walled beams using variational asymptotic methods

Jae-Sang Park and Ji-Hwan Kim

Key Words : Thin-walled beams, Two-cell, Variational asymptotic methods

ABSTRACT

This study investigates the difference between single-cell and multi-cell cross-sections of thin-walled beams. The variationally and asymptotically consistent theory is used in order to model the two-cell thin-walled beam. The theory is based on an asymptotical analysis of two-dimensional shell energy. In addition, the method allows for the development of closed-form expressions for the displacement, stress field and beam stiffness coefficients. The numerical results show the difference between the cross-sectional stiffness of single-cell and that of multi-cell.

1. Introduction

The analysis of a helicopter rotor blade can be separated into a linear two-dimensional analysis of the cross-section and a one-dimensional beam analysis along the blade span. The cross-sectional analysis offers the characteristic properties of the rotor blade for stiffness.

For the cross-section analysis, the cross-section can be modeled as a multi-cell. There have been a few researches for modeling of the cross-section with a multi-cell. Mansfield [1] introduced a flexibility formulation for thin-walled composite beams with two-celled cross-section. The constitutive equation was

derived as a 4×4 matrix including four beam variables such as extension, chordwise/flapwise bendings and torsion. Chandra and Chopra [2] studied the static response of two-cell composite blades through analytical and experimental methods. In their research, 9×9 stiffness matrix considering the transverse shear deformation was derived. Badir [3] developed a variationally and asymptotically consistent theory for two-cell composite beams. The theory gives the closed-form expressions for the displacement, stress field and effective stiffness of the cross-section. The integral actuation using Active Fiber Composites (AFC) and single crystal piezoelectric fiber composites was introduced to Badir's theory [4, 5]. Jung et al. [6] developed the refined structural model for thin- and thick-walled beams.

The most significant difference between the single-cell

* 서울대학교 기계항공공학부

* 서울대학교 기계항공공학부 교수

and multi-cell of cross-sections is in the analysis of torsion. Therefore, this paper shows the difference between the cross-sectional stiffness of single-cell and that of two-cell. Badiř theory [3] is adopted in order to model the two-cell cross-section.

2. Analytical model

2.1 Shell energy functional

Consider the slender two-cell, thin-walled elastic cylindrical shell shown in Fig. 1.

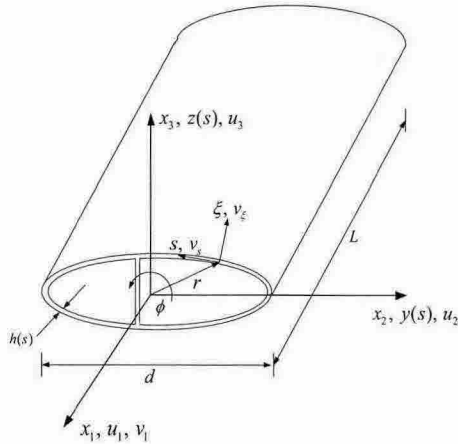


Fig. 1 Two-cell thin-walled beam

It is assumed that

$$\frac{d}{L} \ll 1, \quad \frac{h}{d} \ll 1, \quad \frac{h}{R} \ll 1 \quad (1)$$

By the classical shell theory, the 3D strain energy density can be minimized with respect to ε_{i3} , that is,

$$\hat{U} = \min_{\varepsilon_{i3}} = \frac{1}{2} D^{\alpha\beta\gamma\delta} \varepsilon_{\alpha\beta} \varepsilon_{\gamma\delta} \quad (2)$$

where $D^{\alpha\beta\gamma\delta}$ represents the 2D Hookean tensor.

The two dimensional strain can be expressed as

$$\varepsilon_{\alpha\beta} = \gamma_{\alpha\beta} + \xi \rho_{\alpha\beta} \quad (3)$$

Substituting Eq. (3) into Eq. (2) and integrating over the thickness ξ , the shell energy per unit area of the mid-surface is obtained as

$$2\Phi = \langle D^{\alpha\beta\gamma\delta} \rangle \gamma_{\alpha\beta} \gamma_{\gamma\delta} + 2 \langle D^{\alpha\beta\gamma\delta} \xi \rangle \gamma_{\alpha\beta} \rho_{\gamma\delta} + \langle D^{\alpha\beta\gamma\delta} \xi^2 \rangle \rho_{\alpha\beta} \rho_{\gamma\delta} \quad (4)$$

where the pointed bracket is defined as

$$\langle (\bullet) \rangle = \int_{-h(s)/2}^{h(s)/2} (\bullet) d\xi$$

2.2 Variational asymptotic method

The variational asymptotic method uses an iterative process to model the slender thin-walled shell as a beam. The displacement function corresponding to the zeroth-order approximation is obtained first by minimizing the shell energy functional, Eq. (4) while keeping the leading order terms. In deriving the displacement field, the compatibility condition for warping deformation

$$\oint_i \frac{\partial w_i}{\partial s} ds = 0 \quad (5)$$

is used for each cell i , where w_i represents the out-of-plane warping.

A set of successive corrections is added to the displacement field and the associated energy functional is determined. Corrections generating terms of the same order as previously obtained in the energy functional are kept. The process is terminated when the new corrections do not generate any additional terms of the same order as previously obtained. The second-order approximation is considered in this study.

The displacement field from the second-order approximation becomes

$$\begin{aligned} v_l &= U_1(x) - y(s)U_2'(x) - z(s)U_3'(x) + G(s)\varphi'(x) \\ &\quad + g_1(s)U_1''(x) + g_2(s)U_2''(x) + g_3(s)U_3''(x) \\ v_s &= U_2(x) \frac{dy}{ds} + U_3(x) \frac{dz}{ds} + \varphi(x)r_n \\ v_\xi &= U_2(x) \frac{dz}{ds} - U_3(x) \frac{dy}{ds} - \varphi(x)r_l \end{aligned} \quad (6)$$

where $U_1(x)$, $U_2(x)$ and $U_3(x)$ represent the average cross-sectional translation while $\varphi(x)$ is the torsional rotation. The definition of the other variables for Eq. (6) is summarized Ref. [3, 4].

The strain field associated with Eq. (6) is

$$\begin{aligned} \gamma_{11} &= U_1'(x) - y(s)U_2''(x) - z(s)U_3''(x) \\ 2\gamma_{12} &= \left(\frac{dG}{ds} + r_n \right) \varphi' + \frac{dg_1}{ds} U_1'' + \frac{dg_2}{ds} U_2'' + \frac{dg_3}{ds} U_3'' \\ \gamma_{22} &= 0 \end{aligned} \quad (7)$$

The axial stress resultant N_{11} and the shear stress resultant N_{12} are derived from the shell energy density in Eq. (4) and are given as

$$N_{11} = \frac{\partial \Phi_1}{\partial \gamma_{11}} = A(s)\gamma_{11} + B(s)\gamma_{12}$$

$$\begin{aligned}
N_{12} &= \frac{\partial \Phi_1}{\partial (2\gamma_{12})} = \frac{1}{2} (B(s)\gamma_{11} + C(s)\gamma_{12}) \\
&= \text{constant} \\
N_{22} &= \frac{\partial \Phi_1}{\partial \gamma_{22}} = 0
\end{aligned} \tag{8}$$

The constitutive relationships can be expressed from following equations.

$$\begin{aligned}
F_1 &= \oint \frac{\partial \Phi_2}{\partial (U_1')} ds & M_1 &= \oint \frac{\partial \Phi_2}{\partial (\varphi')} ds \\
M_2 &= \oint \frac{\partial \Phi_2}{\partial (-U_3'')} ds & M_3 &= \oint \frac{\partial \Phi_2}{\partial (U_2'')} ds
\end{aligned} \tag{9}$$

Therefore, the constitutive equation can be represented as a matrix form as follows

$$\begin{Bmatrix} F_1 \\ M_1 \\ M_2 \\ M_3 \end{Bmatrix} = \begin{bmatrix} K_{11} & K_{12} & K_{13} & K_{14} \\ K_{12} & K_{22} & K_{23} & K_{24} \\ K_{13} & K_{23} & K_{33} & K_{34} \\ K_{14} & K_{24} & K_{34} & K_{44} \end{bmatrix} \begin{Bmatrix} U_1' \\ \varphi' \\ -U_3'' \\ U_2'' \end{Bmatrix} \tag{10}$$

where

$$\begin{aligned}
K_{11} &= \oint \left(A - \frac{B^2}{C} \right) ds - 4a_5 \oint_1 \frac{B}{C} ds - 4a_4 \oint_{II} \frac{B}{C} ds \\
K_{12} &= -4a_1 \oint_1 \frac{B}{C} ds - 4a_2 \oint_{II} \frac{B}{C} ds \\
K_{13} &= \oint \left(A - \frac{B^2}{C} \right) z ds + 4a_7 \oint_1 \frac{B}{C} ds + 4a_8 \oint_{II} \frac{B}{C} ds \\
K_{14} &= -\oint \left(A - \frac{B^2}{C} \right) y ds - 4a_5 \oint_1 \frac{B}{C} ds - 4a_6 \oint_{II} \frac{B}{C} ds \\
K_{22} &= -4a_1 A_{eI} - 4a_2 A_{eII}, \quad K_{23} = 4a_7 A_{eI} + 4a_8 A_{eII} \\
K_{24} &= -4a_5 A_{eI} - 4a_6 A_{eII} \\
K_{33} &= \oint \left(A - \frac{B^2}{C} \right) z^2 ds + 4a_7 \oint_1 \frac{B}{C} z ds + 4a_8 \oint_{II} \frac{B}{C} z ds \\
K_{34} &= -\oint \left(A - \frac{B^2}{C} \right) y z ds - 4a_5 \oint_1 \frac{B}{C} z ds - 4a_6 \oint_{II} \frac{B}{C} z ds \\
K_{44} &= \oint \left(A - \frac{B^2}{C} \right) y^2 ds + 4a_5 \oint_1 \frac{B}{C} y ds + 4a_6 \oint_{II} \frac{B}{C} y ds
\end{aligned} \tag{11}$$

where the integral without any subscripts denotes over-all-section evaluation, which is a summation of evaluations over $s=0 \rightarrow s_1$, $s_1 \rightarrow s_2$ and $s_2 \rightarrow s_3$ (Fig. 2). In addition, the diagonal terms K_{11} , K_{22} , K_{33} and K_{44} represent EA , GJ , EI_y and EI_z of a blade, respectively.

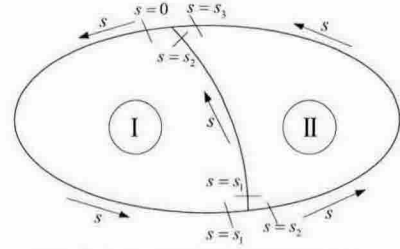


Fig. 2 Branches for integration of a two-cell thin-walled beam

3. Result and discussion

3.1 Code verification

To verify the codes used in this study, a two-cell composite box beam is considered (Fig. 3). The material properties of AS4/3506-1 Graphite/epoxy are given as

$$\begin{aligned}
E_1 &= 142 \text{ GPa} & E_2 &= 9.8 \text{ GPa} \\
G_{12} &= 6.0 \text{ GPa} & \nu_{12} &= 0.3 \\
\text{Thickness} &= 1.270 \times 10^{-4} \text{ m}
\end{aligned}$$

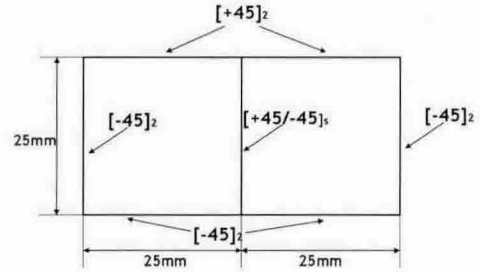


Fig. 3 Two-cell thin-walled composite box beam

Table 1 shows that the present result has reasonable correlation with the previous result [7]. The difference in the values for K_{13} can be explained by a difference in sign between the integral expressions.

Table 1 Non-zero stiffness results for two-cell composite box beam (N, N-m, N-m²)

K_{ij}	Present	Ref. [7]
K_{11}	8.519×10^5	8.477×10^5
K_{12}	-1.850×10^3	-1.794×10^3
K_{13}	-6.472×10^2	6.337×10^2
K_{22}	1.322×10^2	1.278×10^2
K_{23}	4.624×10^1	4.461×10^1
K_{33}	9.818×10^1	9.567×10^1
K_{44}	2.094×10^2	2.070×10^2

3.2 Comparison between cross-sectional stiffness of two-cell and single cell

This section studies the comparison between cross-sectional stiffness of two- and single-cell models. Fig. 4 shows the two-cell composite blade section with a NACA0012 airfoil. The cross-section of a blade consists of nose, spar, web and fairing. Material properties for E-glass used in this example are

$$\begin{aligned} E_1 &= 14.8 \text{ GPa} & E_2 &= 13.6 \text{ GPa} \\ G_{12} &= 1.9 \text{ GPa} & \nu_{12} &= 0.19 \\ \rho &= 1800 \text{ kg/m}^3 & \text{Thickness} &= 2.032 \times 10^{-4} \text{ m} \end{aligned}$$

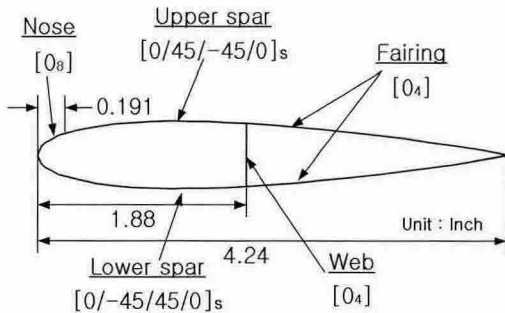


Fig. 4 Two-cell composite blade cross-section

Table 2 represents the cross-sectional stiffness of two- and single-cell models. The single-cell model can be obtained from ignoring the web of a two-cell model. As shown in Table 2, the axial stiffness EA and two bending stiffness EI_y and EI_z of a two-cell model are slightly higher than those of a single-cell model, however the torsional stiffness GJ of a two-cell model is about 1.85 times that of a single-cell model. Thus, the difference in the torsional stiffness between two- and single-cell models has to be considered in the cross-sectional analysis in order to perform vibration and aeroelastic analyses of a rotor blade, efficiently.

Table 2 Cross-sectional properties of two- and single-cell models

	Two-cell model	Single-cell model
EA (N)	3.462×10^6	3.317×10^6
GJ (N-m ²)	6.069×10^1	3.779×10^1
EI_y (N-m ²)	8.083×10^1	7.906×10^1
EI_z (N-m ²)	4.677×10^3	4.614×10^3

4. Conclusions

This study shows the difference between the cross-sectional stiffness of two- and single-cell cross-section models. The cross-sectional analysis is performed through the variationally and asymptotically consistent theory. The result represents that the torsional stiffness of a two-cell model is higher than that of a single-cell model.

Acknowledgement

This work was supported by Korea research Foundation Grant (KRF-2004-041-D00039).

References

- (1) Mansfield, E. H., "The stiffness of a two-cell anisotropic tube," *Aeronautical Quarterly*, May 1981, pp. 338-353
- (2) Chandra, R., and Chopra, I., "Structural behavior of two-cell composite rotor blades with elastic couplings," *AIAA Journal*, Vol. 30, No. 12, 1992, pp. 2914-2921
- (3) Badir, A. M., "Analysis of two-cell composite beams," *Proceedings of the 36th Structures, Structural Dynamics and Materials Conference*, New Orleans, LA, April 10-12, 1995, pp. 419-424
- (4) Cesnik, C. E. S., and Shin, S. J., "On the modeling of integrally actuated helicopter blades," *International Journal of Solids and Structures*, Vol. 38, 2001, pp. 1765-1789
- (5) Park, J. -S., and Kim, J. H., "Cross sectional analysis of helicopter rotor blades incorporating single crystal piezoelectric fiber composite actuators," *Proceedings of the Korean Society for Aeronautical and Space Sciences Fall Conference*, 2005
- (6) Jung, S. N., Nagaraj, V. T. and Chopra, I., "Refined structural model for thin- and thick- walled composite rotor blades," *AIAA Journal*, Vol. 40, No. 1, 2002, pp. 105-116
- (7) Cesnik, C. E. S., and Hodges, D. H., "VABS: A new concept for composite rotor blade cross-sectional modeling," *Journal of American Helicopter Society*, Vol. 42, 1997, pp. 27-38